© 2015. Published by The Company of Biologists Ltd | Development (2015) 142, 681-691 doi:10.1242/dev.114850

RESEARCH ARTICLE

Mitochondrial dysfunction in oocytes of obese mothers: transmission to offspring and reversal by pharmacological endoplasmic reticulum stress inhibitors

Linda L. Wu[1], Darryl L. Russell[1], Siew L. Wong[1], Miaoxin Chen[1], Te-Sha Tsai[2], Justin C. St John[2], Robert J. Norman[1], Mark A. Febbraio[3], John Carroll[4] and Rebecca L. Robker[1,*]

ABSTRACT

Over-nutrition in females causes altered fetal growth during pregnancy and permanently programs the metabolism of offspring; however, the temporal and mechanistic origins of these changes, and whether they are reversible, are unknown. We now show that, in obese female mice, cumulus-oocyte complexes exhibit endoplasmic reticulum (ER) stress, high levels of intracellular lipid, spindle abnormalities and reduced PTX3 extracellular matrix protein production. Ovulated oocytes from obese mice contain normal levels of mitochondrial (mt) DNA but have reduced mitochondrial membrane potential and high levels of autophagy compared with oocytes from lean mice. After *in vitro* fertilization, the oocytes of obese female mice demonstrate reduced developmental potential and form blastocysts with reduced levels of mtDNA. Blastocysts transferred to normal weight surrogates that were then analyzed at E14.5 showed that oocytes from obese mice gave rise to fetuses that were heavier than controls and had reduced liver and kidney mtDNA content per cell, indicating that maternal obesity before conception had altered the transmission of mitochondria to offspring. Treatment of the obese females with the ER stress inhibitor salubrinal or the chaperone inducer BGP-15 before ovulation increased the amount of the mitochondrial replication factors TFAM and DRP1, and mtDNA content in oocytes. Salubrinal and BGP-15 also completely restored oocyte quality, embryo development and the mtDNA content of fetal tissue to levels equivalent to those derived from lean mice. These results demonstrate that obesity before conception imparts a legacy of mitochondrial loss in offspring that is caused by ER stress and is reversible during the final stages of oocyte development and maturation.

KEY WORDS: BGP-15, ER stress, Mitochondria, mtDNA, Obesity, Ovary

INTRODUCTION

Over-nutrition in females, including humans, re-programs offspring metabolism, causing altered fetal and postnatal growth trajectories (Srinivasan et al., 2006; Samuelsson et al., 2008; Shankar et al., 2008; Rattanatray et al., 2010; Ruager-Martin et al., 2010; Yan et al., 2011). Studies in rodent obesity models have demonstrated that maternal over-nutrition contributes at very early stages to offspring metabolic programming through altering the periconception oocyte and development of the pre-implantation embryo (Minge et al., 2008; Igosheva et al., 2010; Jungheim et al., 2010; Wu et al., 2010; Shankar et al., 2011; Luzzo et al., 2012). Impaired fertility also commonly occurs with obesity; for instance, overweight women often require assisted reproductive technologies, such as *in vitro* fertilization (IVF), and their success rates are lower, owing to poor oocyte developmental potential (Cardozo et al., 2011). However, the fundamental mechanisms in the oocyte and pre-implantation embryo that are changed by maternal over-nutrition, determining fertility potential and establishing the metabolic phenotype of the offspring, are unknown.

Our previous studies have demonstrated that mouse cumulus oocyte complexes (COCs) exhibit lipotoxicity responses in association with obesity or following treatment with high levels of lipids *in vitro* (Wu et al., 2010, 2012). Lipotoxicity is a cellular response to a high lipid extracellular environment, including high levels of triglyceride, cholesterol and/or free fatty acids, which increase intracellular lipid accumulation and damage organelles, particularly endoplasmic reticulum (ER) and mitochondria (Schaffer, 2003; Borradaile et al., 2006). Impaired ER function, or ER stress, disrupts protein secretion pathways and triggers the unfolded protein response (UPR) (Kaufman, 1999; Ozcan and Tabas, 2012) – adaptive mechanisms to restore protein folding, particularly in secretory cells. In parallel, Ca^{2+} released from the ER disrupts mitochondrial membrane potential and increases production of reactive oxygen species (ROS), triggering oxidative stress (Malhotra and Kaufman, 2007; Vannuvel et al., 2013). These stressors initiate compensatory survival responses, such as the induction of protein-folding chaperones and autophagy to remove aggregated proteins and damaged organelles; however, if homeostasis is not achieved, cells ultimately undergo apoptosis (Kim et al., 2008; Shore et al., 2011). In mice that have been fed high fat diets, oocytes accumulate lipid, exhibit markers of ER stress and increased ROS, and have altered mitochondrial ultrastructure and membrane potential (Igosheva et al., 2010; Wu et al., 2010; Luzzo et al., 2012). We hypothesize that these disruptions to oocyte organelles are linked and that ER stress underpins the impact of obesity on oocyte developmental potential and offspring metabolism.

Mitochondria are essential for the generation of ATP during oocyte maturation and blastocyst formation (Van Blerkom et al., 1995; Dumollard et al., 2007). Studies using mice lacking TFAM, a nuclear-encoded mitochondrial (mt)DNA replication factor, demonstrate that oocytes must contain threshold numbers of mitochondria, with 40,000 to 50,000 copies of mtDNA, in order for an embryo to give rise to a viable fetus (Wai et al., 2010). Furthermore, because oocyte-derived

[1]School of Paediatrics and Reproductive Health, Robinson Research Institute, The University of Adelaide, Adelaide, SA, 5005, Australia. [2]Centre for Genetic Diseases, MIMR-PHI Institute of Medical Research, and Department of Molecular and Translational Science, Monash University, Clayton, VIC, 3168, Australia. [3]Cellular and Molecular Metabolism Laboratory, Baker IDI Heart and Diabetes Institute, Melbourne, VIC, 3004, Australia. [4]School of Biomedical Sciences, Nursing and Health Sciences, Monash University, Clayton, VIC, 3800, Australia.

*Author for correspondence (Rebecca.robker@adelaide.edu.au)

Received 27 June 2014; Accepted 15 December 2014

Development (2015) 142, 681-691 doi:10.1242/dev.114850

mitochondria give rise to the entire complement of mitochondria in offspring tissues, their transmission, replication and inheritance are tightly regulated. Post fertilization, oocyte-derived mitochondria are segregated into each embryonic daughter cell until the blastocyst stage, at which point the pluripotent inner-cell-mass cells establish a threshold mtDNA set-point, from which they commence mtDNA replication in a differentiation-specified manner (St John, 2012). Whether this process is disrupted in oocytes from obese animals, and its potential contribution to altered offspring metabolism, has not been tested.

In this study, we sought to determine whether ER stress is responsible for altering oocyte mitochondrial activity and developmental potential, and whether this changes the embryonic mitochondrial set-point that is transmitted to the developing fetus. We recapitulated obesity and metabolic syndrome from excessive consumption using a mouse model of Alstrom syndrome (a rare human genetic disease that causes hyperphagia leading to severe obesity, hyperinsulinemia and ultimately diabetes) (Girard and Petrovsky, 2011). Mouse lines with mutations in the *Alms1* gene, either the spontaneous 'Fat Aussie' (*Alms1*^{foz}/*Alms1*^{foz}) strain or the N-ethyl-N-nitrosourea (ENU)-induced 'Blobby' strain (*Alms1*^{bbb}/*Alms1*^{bbb}), overeat and develop severe obesity on standard low-fat mouse chow, avoiding confounding issues of dietary composition. We examined lipotoxicity responses, particularly ER stress, protein production and mitochondrial dysfunction, in the COCs of obese Blobby (*Alms1*^{bbb}/*Alms1*^{bbb}) mice and compared them with those of non-obese littermates. Subsequently, the developmental potential of oocytes of obese mice was monitored following IVF, and the fetal mtDNA content was measured following uterine transfer.

Importantly, we tested the ability of two pharmaceutical compounds (known to alleviate ER stress via different pathways) to reverse the effects of obesity on oocytes and to restore embryo development. Salubrinal, a selective eIF2α dephosphorylation inhibitor, is a well-characterized ER stress inhibitor that acts by maintaining phosphorylated eIF2α and upregulation of its downstream mediators, such as transcription factor *Aft4* and chaperone protein *Hspa5*, thereby prolonging the protein kinase RNA-like ER kinase (PERK) branch of the UPR pathway and restoring ER homeostasis (Boyce et al., 2005; Sokka et al., 2007; Tian et al., 2011; Kuo et al., 2012). BGP-15 is a hydroximic acid derivative that is a potent inducer of the chaperone HSP72 (*Hspa1a*/*Hspa1b*) and that, in muscle, increases sarcoplasmic and/or endoplasmic reticulum Ca^{2+}ATPase (SERCA) activity (Gehrig et al., 2012) and protects against obesity-induced insulin resistance (Chung et al., 2008). The results show that both compounds restore mitochondrial activity in oocytes from obese mice, and normalize embryo development and fetal mtDNA transmission.

RESULTS

Blobby mice exhibit obesity, hyperinsulinemia and dyslipidemia on a chow diet

Female *Alms1* mutant mice anecdotally exhibit infertility following the onset of obesity (Arsov et al., 2006) (Australian Phenome Bank, personal communication); however, the underlying reason for this infertility is unknown. We used the Blobby (*bbb/bbb*) mouse strain to characterize the metabolic defects in females and to determine whether there are defects in ovulation and/or oocyte quality that contribute to their obesity-induced sub-fertility. Female Blobby mice developed significantly increased body weights relative to wild-type and heterozygous littermates from 5 weeks of age (Blobby, 18.4±0.3 g; wild type, 17.1±0.2 g; heterozygous, 16.7±0.2 g; P=0.0002, one-way ANOVA at week 5). This excessive weight gain increased progressively with age (Fig. 1A), such that at 14 weeks of age, Blobby mice weighed 36.0±0.5 g, whereas the average weight of wild-type littermates was 23.6±0.6 g and that of heterozygotes was 22.7±0.5 g (Fig. 1A; P<0.0001, one-way ANOVA at week 14). Thus, at 14 weeks of age, Blobby mice weighed on average 12.5 g, or 53%, more than wild-type littermates (Fig. 1B). This increased body weight was associated with a 230% increase in abdominal adipose tissue mass (Fig. 1C) and a 53% increase in liver mass (Fig. 1D). The Blobby mice also had significantly higher levels (9.7-fold) of circulating insulin than wild-type littermates (Fig. 1E), indicating insulin resistance, but circulating glucose was not different (Fig. 1F). Cholesterol,

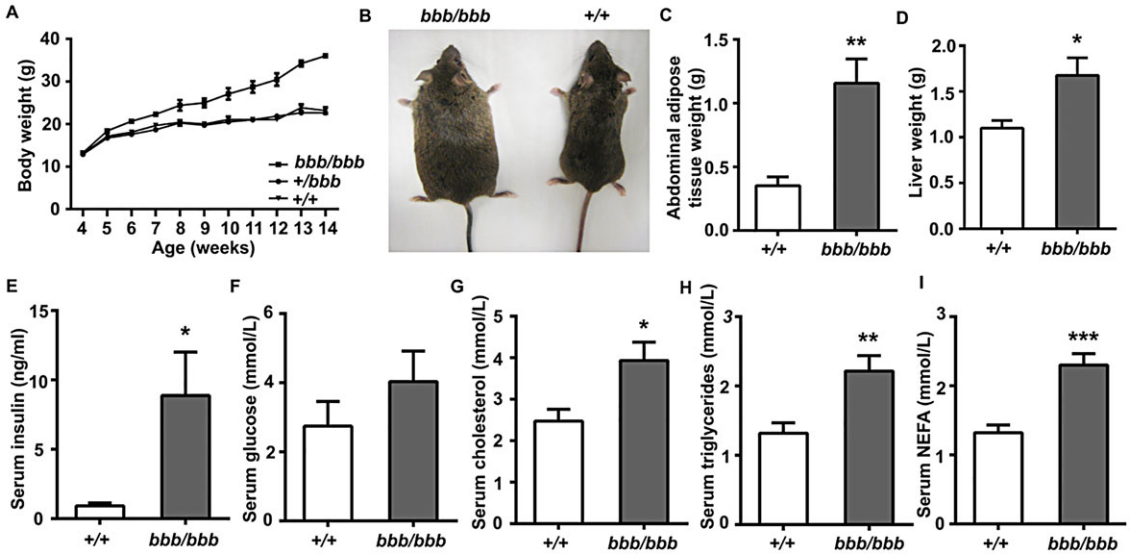

Fig. 1. Blobby mice exhibit obesity, hyperinsulemia and dyslipidemia on a chow diet. (A) The body weights of female wild-type (+/+; n=13), heterozygous (+/*bbb*; n=17) and Blobby (*bbb*/*bbb*; n=12) mice maintained on standard chow diet from 4 to 14 weeks of age. Blobby mice are significantly heavier than +/+ and +/*bbb* littermates from 5 weeks of age (one-way ANOVA, Tukey's post hoc test; P<0.01 from 5 weeks). (B) A 14-week-old Blobby mouse (left) and wild-type littermate (right). Tissue weight of abdominal adipose tissue (C) and liver (D). Serum insulin (E), glucose (F), cholesterol (G), triglycerides (H) and non-esterified fatty acids (NEFA) (I). +/+, n=13; Blobby, n=13; data are presented as means+s.e.m.; *P<0.05, **P<0.01, ***P<0.0001, calculated using Student's t-test.

Development (2015) 142, 681-691 doi:10.1242/dev.114850

triglycerides and free fatty acids were also significantly higher (60-74% increased) in Blobby females compared with that of wild-type littermates (Fig. 1G-I). These data demonstrate that Blobby female mice develop hyperinsulinemia and hyperlipidemia by 14 weeks of age, whereas hyperglycemia is not evident.

Ovulatory dysfunction in obese mice is reversed by ER stress inhibitors

When treated with ovulatory gonadotropins, the ovaries of Blobby mice often exhibited non-ovulated follicles, which were rarely observed in non-obese wild-type and heterozygous littermates (Fig. 2A; supplementary material Fig. S1). The number of ovulated COCs found in the oviduct was significantly reduced in Blobby mice compared with non-obese littermates (Fig. 2B). At 6 weeks of age, Blobby mice were on average just 1.5 g heavier than wild-type and heterozygous littermates (see Fig. 1A), and ovulation following treatment with gonadotropins was not impaired (Fig. 2B, right panel), demonstrating that impaired oocyte release in Blobby mice is due to obesity rather than the *Alms1* mutation. Treatment of mice with either salubrinal (1 mg/kg) or BGP-15 (100 mg/kg) once daily for 4 days increased the ovulation rate with a significant improvement in response to BGP-15, particularly in obese Blobby mice, where the ovulation rate was more than doubled from an average of 7.5 to 18.8 oocytes per mouse (Fig. 2B). The ability of BGP-15 to increase the ovulation rate in lean mice was verified in additional 8-week-old C57 mice (supplementary material Fig. S2). Treatment of mice (lean or obese) with salubrinal or BGP-15 had no effect on body weight (data not shown).

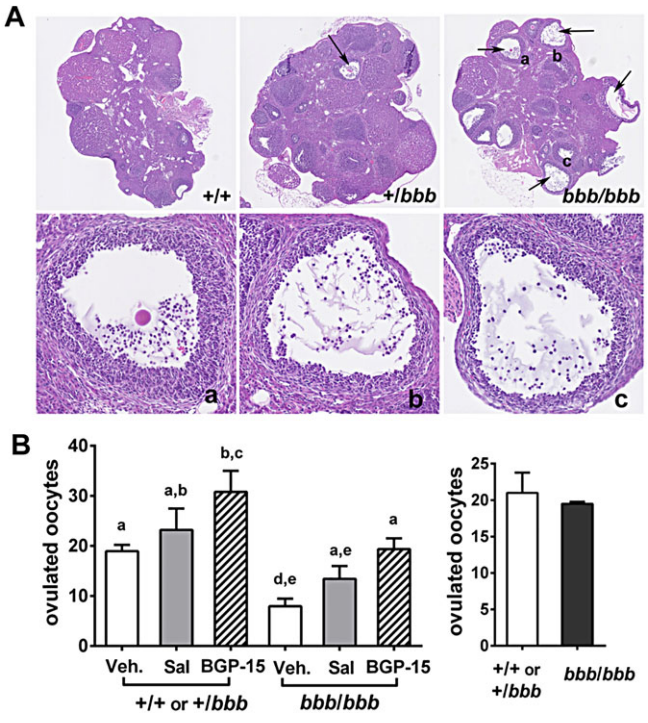

Fig. 2. Ovulation rate declines with increasing body weight but is improved by treatment with ER stress inhibitors. (A) Hematoxylin and Eosin-stained ovary sections from 14-week-old gonadotropin-treated lean (+/+ or +/*bbb*) and obese Blobby (*bbb*/*bbb*) mice. Arrows indicate unruptured follicles, which are prevalent in ovaries from obese mice. Representative examples from *n*=4 mice per genotype are shown. Panels a-c are higher magnifications of the indicated follicles of the Blobby mouse. (B) The number of ovulated oocytes in 14-week-old lean and obese mice treated with saline vehicle (Veh.), salubrinal (Sal) or BGP-15 i.p. once per day for 4 days. Values are means+s.e.m. (lean mice+Veh, *n*=19; lean+Sal, *n*=5; lean+BGP-15, *n*=10; obese mice+Veh, *n*=22; obese+Sal, *n*=16; obese+BGP-15, *n*=14). Different letters indicate significant differences calculated by one-way ANOVA, Tukey's post hoc test; $P<0.0001$. Right panel: the number of ovulated oocytes in oviducts is not reduced in *bbb*/*bbb* mice prior to the onset of obesity, at 6 weeks of age (+/+; +/*bbb*: *n*=11; *bbb*/*bbb* *n*=4; Student's *t*-test).

Oocyte complexes in obese mice exhibit gene expression and protein changes associated with ER stress

To determine whether ER stress occurs in COCs of obese Blobby mice on a standard diet, similar to that of COCs of mice fed a high fat diet (Wu et al., 2010), the mRNA expression of ER stress markers [*Aft4*, *Atf6* and the spliced *Xbp1* transcript (*Xbp1*s)] and chaperones (*Hspa5*, *Hspa1a* and *Hspa1b*) was measured in ovulated COCs and granulosa-lutein cells of gonadotropin-treated 14-week-old Blobby mice and compared with those of wild-type and heterozygous littermates. Ovulated COCs from Blobby mice had significantly increased expression of *Atf4*, *Hspa1a* and *Hspa1b* compared with wild-type littermates (Fig. 3), and tended to have higher expression levels of *Atf6* (not shown) and *Xbp1*s, reflective of

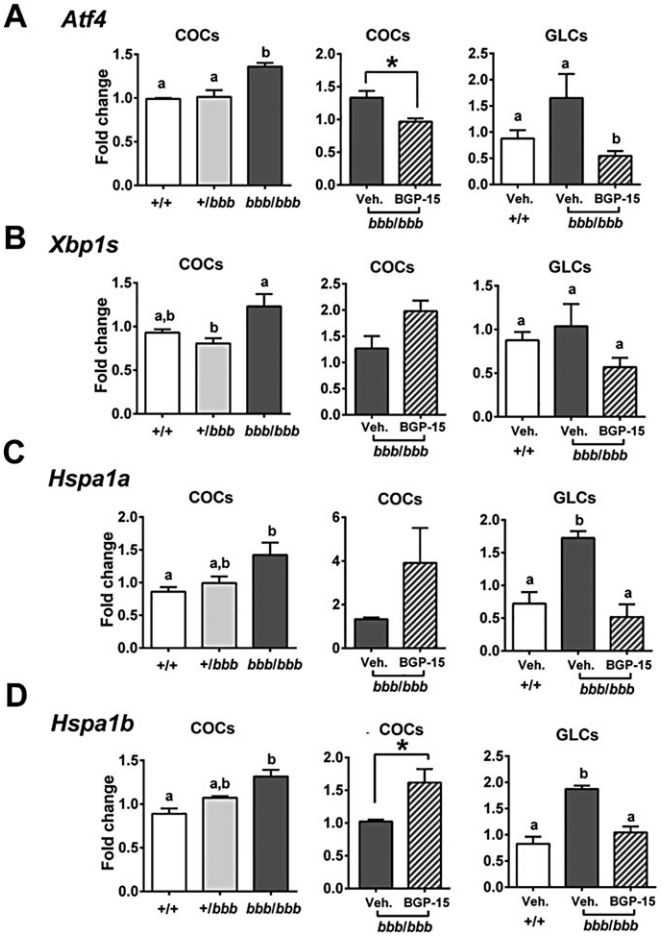

Fig. 3. ER stress and UPR marker genes in COCs and granulosa-lutein cells are affected by obesity and BGP-15. Ovulated COCs were collected from oviducts and granulosa-lutein cells that had been dissected from ovaries of gonadotropin-treated lean (+/+ or +/*bbb*) or obese (*bbb*/*bbb*) mice, or obese mice that had been treated with BGP-15. Expression of ER stress and UPR marker genes [*Atf4* (A) and *Xbp1*s (B)], and heat shock chaperone genes [*Hspa1a* (C) and *Hspa1b* (D)] were determined by using RT-PCR. Data are presented as means+s.e.m. and expressed as fold changes compared with a calibrator sample; *n*=3-6 RNA samples per genotype with each sample a pool of cells from four mice. Different letters indicate significant differences ($P<0.05$) calculated by one-way ANOVA; *$P<0.05$ calculated by Student's *t*-test.

Development (2015) 142, 681-691 doi:10.1242/dev.114850

activation of the UPR. COCs from obese mice that had been treated with BGP-15 had significantly decreased expression of *Atf4* but increased expression of *Xbp1*s, *Hspa1a* and *Hspa1b* (Fig. 3). Similar effects were observed in granulosa-lutein cells that were isolated at the same timepoint as the COCs. Cells from obese Blobby mice had significantly increased expression of *Hspa1a* and *Hspa1b* (Fig. 3), and tended to have higher expression of *Atf4*, *Xbp1*s and *Atf6* (not shown). Similarly, treatment with BGP-15 decreased *Atf4* expression in granulosa-lutein cells and, interestingly, also reduced the expression of *Xbp1*s, *Hspa1a* and *Hspa1b*. The induction of ER stress marker genes in the Blobby mice occurred in association with obesity, and they were not different in the COCs or granulosa-lutein cells of young lean mice (supplementary material Fig. S3).

Increased accumulation of lipid droplets and impaired protein production and secretion are additional key characteristics of lipotoxic induction of the UPR and ER stress. We thus measured these parameters in ovulated COCs of obese Blobby mice and lean littermates, and determined whether the defects were reversible with the ER stress inhibitor salubrinal *in vivo*. Oocytes of obese Blobby mice had visibly more lipid (green fluorescence) than oocytes from lean littermates, and treatment with salubrinal for 4 days before ovulation did not significantly affect lipid levels within the oocytes (Fig. 4A,B). Extracellular matrix protein pentraxin-3 (PTX3), which is crucial for fertilization (Varani et al., 2002; Salustri et al., 2004), was measured by using immunocytochemistry and showed an abundance of secreted PTX3 (red fluorescence) in the extracellular matrix of COCs from lean mice. COCs from obese Blobby mice had very low levels of detectable PTX3 protein in the cumulus matrix, but Blobby mice that had been treated with salubrinal showed restoration of strong PTX3 staining in cumulus matrix, similar to that of the lean controls (Fig. 4A,C; supplementary material Fig. S4). Thus, *in vivo* treatment with ER stress inhibitors does not markedly affect oocyte lipid content but normalizes PTX3 protein production.

Denuded oocytes were also examined for spindle morphology and chromosomal alignment. Oocytes from obese Blobby mice exhibited an increased incidence of abnormalities that were consistent with previous observations in obese mice and humans (Luzzo et al., 2012; Machtinger et al., 2012). Mice that had been treated with BGP-15 exhibited normalized spindle morphology and chromosome alignment (Fig. 4D,E).

Oocytes in obese mice exhibit reduced mitochondrial membrane potential and autophagy

We next determined whether the oocyte mitochondrial membrane potential ($\Delta\Psi$m) was reduced in ovulated oocytes from obese Blobby mice by staining with the inner membrane potential dye 5,5′,6,6′-tetrachloro-1,1′,3,3′-tetraethylbenzimidazolylcarbocyanine iodide (JC-1). Consistent with previous reports (Van Blerkom et al., 2002; Wu et al., 2010), oocytes of ovulated COCs exhibited red punctuate fluorescence that was localized to the pericortical region, indicating a high $\Delta\Psi$m, whereas green fluorescence, indicating a low $\Delta\Psi$m, localized to the central cytoplasm of oocytes (Fig. 5A). In oocytes from obese mice, the red punctuate fluorescence in the pericortical region was visibly reduced compared to that of oocytes from non-obese littermates. Oocytes from Blobby mice that had been treated with salubrinal for 4 days before ovulation did not have reduced punctuate fluorescence in the pericortical region. Analysis of the ratio of red to green fluorescence intensity, in order to generate an index of mitochondrial activity, provided further evidence that the significantly decreased mitochondrial activity in

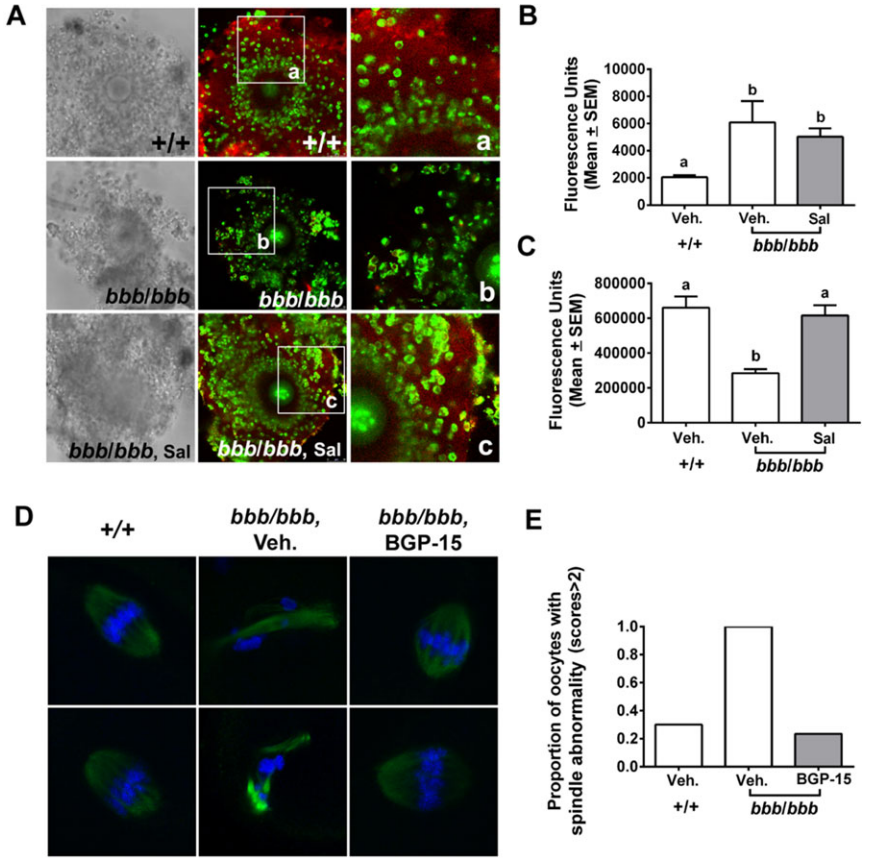

Fig. 4. COCs from obese mice have reduced secretion of extracellular matrix protein PTX3 and spindle abnormalities that are normalized after treatment with an ER stress inhibitor. Ovulated COCs obtained from oviducts 13 h after ovulatory gonadotropin treatment were (A) stained with neutral lipid dye BODIPY 493/503 (green fluorescence) and for cumulus matrix protein PTX3 by using immunocytochemistry (red fluorescence). The left-hand panels are brightfield photomicrographs of labeled COCs (center panels), and the right-hand panels are higher magnification images of the boxed areas. Images are representative of 10-15 COCs from two to three mice per group. (B) Oocyte lipid content was calculated as the total green fluorescence within each oocyte. (C) PTX3 levels were calculated as the total red fluorescence within each COC. Veh=vehicle treated. *n*=10-15 per group. Different letters indicate significant difference calculated by one-way ANOVA, Tukey's post hoc test; $P<0.0001$. (D) Denuded oocytes were immunostained for tubulin (green) and with Hoechst 33342 (blue) to visualize spindle morphology which was assessed in (E) *n*=14-34 oocytes per group; $P<0.0001$ by chi-square.

Development (2015) 142, 681-691 doi:10.1242/dev.114850

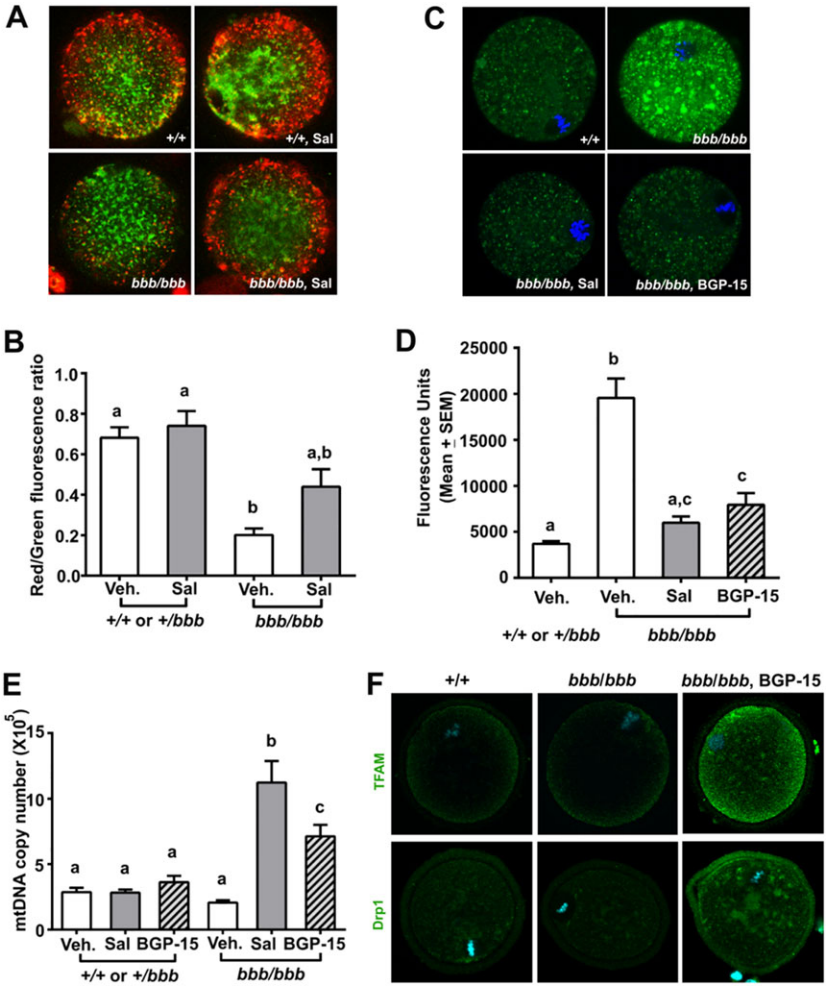

Fig. 5. Treatment with salubrinal or BGP-15 induces mtDNA replication and normalizes mitochondrial membrane potential (ΔΨm) and autophagy in oocytes from obese mice. Obese mice (*bbb*/*bbb*) or lean littermates (+/+ or +/*bbb*) were treated with vehicle (Veh), salubrinal (Sal) or BGP-15 i.p. once daily for 4 days, and oocytes were collected from the oviducts. (A) Live oocytes stained with JC-1, where red fluorescence indicates high ΔΨm, and green indicates low ΔΨm. (B) Ratio of red to green fluorescence, an indicator of mitochondrial activity. Data are presented as means+s.e.m., *n*=6-30 oocytes from four mice per group. (C) Live oocytes were assessed for autophagic vacuoles, visualized as green fluorescence. Hoechst 33342 (blue). (D) Autophagy levels were quantified as the sum total of green fluorescence within each oocyte. Data are presented as means+s.e.m., *n*=8-10 oocytes from three mice per group. (E) mtDNA copy number in individual oocytes collected from treated mice. Data are presented as means+s.e.m.; *n*=19-38 oocytes from six mice per group over three independent experiments. (F) Representative examples of oocytes from three or four mice per treatment group immunostained for TFAM or DRP1 (green) and Hoechst 33342 (blue). Different letters indicate significant differences calculated by one-way ANOVA, Tukey's post hoc test, $P<0.0001$.

ovulated oocytes from obese mice was reversed by treatment with salubrinal (Fig. 5B). Induction of autophagy was also measured in oocytes by using an activity assay, and this showed that oocytes from obese mice exhibited numerous autophagic vacuoles throughout the oocyte cytoplasm (Fig. 5C). Quantification confirmed that levels were fourfold higher in oocytes from obese mice compared with those of lean littermates (Fig. 5D). Furthermore, the treatment of obese mice with either salubrinal or BGP-15 significantly diminished autophagic activity (Fig. 5C,D).

As another measure of mitochondrial capacity, mtDNA copy number was quantitatively assessed in individual oocytes. Oocytes from obese Blobby mice had a small reduction in mtDNA copy number that was not statistically significant (Fig. 5E), in contrast to previous reports (Igosheva et al., 2010; Luzzo et al., 2012). The treatment of obese mice with salubrinal or BGP-15 resulted in a dramatic increase in oocyte mtDNA, which was not observed in lean littermates that had been treated with either compound. To further investigate how salubrinal and BGP-15 increase mtDNA in oocytes, we measured the expression of the mtDNA transcription factor TFAM and mitochondrial fission marker DRP1, and found that oocytes from obese Blobby mice that had been treated with either drug exhibited dramatically higher levels of both TFAM and DRP1 than either untreated obese mice or their lean littermates (Fig. 5F). The effects of BGP-15 on oocyte mitochondria were verified in a mouse model of high fat diet-induced obesity where, again, the oocytes of obese mice exhibited reduced mitochondrial activity that was normalized after treatment with BGP-15, which also significantly induced mtDNA copy number (supplementary material Fig. S5).

Poor oocyte developmental competence and skewed fetal growth in obese mice are alleviated after treatment with an ER stress inhibitor

Ovulated oocyte complexes that had been collected from oviducts were fertilized *in vitro*, and oocyte viability and embryo development were compared to those of untreated obese and lean control littermates. At 4 h post fertilization, many oocytes (putative zygotes) from untreated obese mice underwent fragmentation (Fig. 6A, arrows) and were deemed non-viable. The percentage of viable oocytes was significantly lower in obese mice than in lean mice, but treatment of obese mice with salubrinal or BGP-15 reversed this defect, and these treated mice had similar proportions of healthy viable oocytes to those of lean mice (Fig. 6A,B). The morphologically viable oocytes and/or zygotes from obese Blobby mice were further monitored, and they exhibited a significantly lower cleavage rate on day 2 compared to those from lean mice (Fig. 6C), and this was normalized in salubrinal-treated and BGP-15-treated obese mice. The percentage of blastocysts that developed from two-cell embryos of obese Blobby mice was further reduced (Fig. 6D) compared with that of lean mice, and development rates were normalized by using salubrinal or BGP-15. These defects in embryo development are specifically due to maternal obesity because ovulated oocytes from 6-week-old *bbb*/*bbb* mice, when assessed in an identical way, showed development

Development (2015) 142, 681-691 doi:10.1242/dev.114850

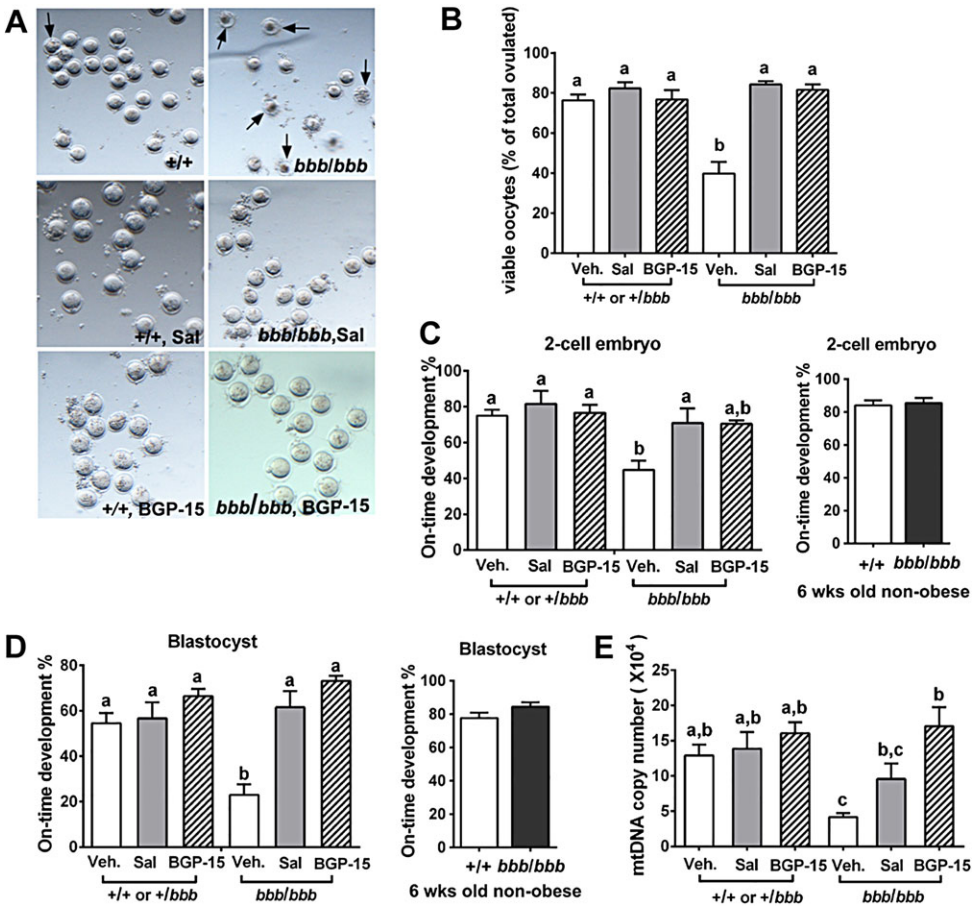

Fig. 6. Oocytes from obese Blobby mice exhibit impaired embryo development that is restored by treatment with salubrinal or BGP-15. Obese Blobby (*bbb*/*bbb*) mice or lean littermates (+/+ or +/*bbb*) at 14 weeks of age (except where indicated) were treated with vehicle (Veh; saline), salubrinal (Sal) or BGP-15 daily for 4 days. Ovulated oocytes were collected from oviducts 16 h following hCG injection and fertilized *in vitro*. (A) At 4 h after *in vitro* fertilization, many degenerate oocytes (arrows) from untreated obese mice were observed. (B) The percentage of viable oocytes presented as means+s.e.m. Embryo development was assessed on day 2 and day 5 following IVF and is presented as the mean percentage of embryos exhibiting appropriate ('on-time') development+s.e.m. (C) Two-cell embryos developed from viable oocytes by day 2. (D) Blastocysts developed from two-cell embryos by day 5. Lean, n=24; lean+Sal, n=7; lean+BGP-15, n=6; Blobby, n=15; Blobby+Sal, n=6; Blobby+BGP-15, n=7 pools of oocytes from animals within same group. [C,D, right-hand panels are identical assessments of oocytes from 6-week-old (non-obese) mice. +/+, n=13; Blobby, n=10.] (E) Blastocysts were collected at day 5 and the mtDNA copy number of individual blastocysts was measured by using quantitative PCR. Data are expressed as mean copy number+s.e.m.; lean, n=22 blastocysts; lean+Sal, n=10 blastocysts; lean+BGP-15, n=7 blastocysts; Blobby, n=14 blastocysts; Blobby+Sal, n=10 blastocysts; Blobby+BGP-15, n=7 blastocysts collected from three independent IVF experiments. Different letters indicate significant differences by one-way ANOVA, Tukey's post hoc test; P<0.0001.

rates comparable to those of control littermates (Fig. 6C,D, right panels).

mtDNA copy number was reduced in the blastocysts derived from the oocytes of obese Blobby mice compared with blastocysts derived from lean littermates. Blastocyst mtDNA content was normalized after treatment with either salubrinal or BGP-15 for 4 days before ovulation (Fig. 6E). Thus, alterations in the oocytes of obese mice lead to a sustained loss of mitochondria in blastocysts that is potentially attributable to ER stress.

Additional cohorts of blastocysts that were generated by IVF of oocytes from obese Blobby mice or lean wild-type littermates were transferred to the uterus of non-obese recipient mice. There were no differences in the implantation rates between embryos generated from any of the treatment groups (data not shown). Fetuses that developed from the oocytes of obese Blobby mice were significantly heavier than those developed from the oocytes of lean littermates (Fig. 7A). By contrast, fetuses that developed from the oocytes of salubrinal-treated or BGP-15-treated obese mice were no longer significantly heavier than fetuses from wild-type oocytes (Fig. 7A). There was no difference in the placental weights of fetuses from the oocytes of obese mice (or obese mice that had been treated with salubrinal or BGP-15) compared to fetuses derived from wild-type oocytes (data not shown).

mtDNA copy number was measured in dissected fetal tissues and was not found to be different in the placentas of any of the treatment groups (data not shown). However, mtDNA content was significantly reduced in the liver and kidney, and a trend towards a reduction in the hearts of fetuses derived from oocytes of obese females was evident (Fig. 7). Treatment of obese Blobby mice with salubrinal or BGP-15 before IVF resulted in restored mtDNA levels in the tissues of the offspring that had been derived from the oocytes of obese mothers to levels that were not significantly different to those of offspring of non-obese controls. To determine whether mitochondrial DNA sequence, i.e. variant load, was affected in fetal tissues, in addition to copy number, next-generation sequencing was performed on the liver samples from each treatment group. There were 56.75±5.9 rearrangements in the mitochondrial genome of livers from offspring conceived from obese mouse oocytes, which was significantly higher (P<0.01) than the level of 37.50±1.4 mtDNA rearrangements in liver samples from control offspring

Development (2015) 142, 681-691 doi:10.1242/dev.114850

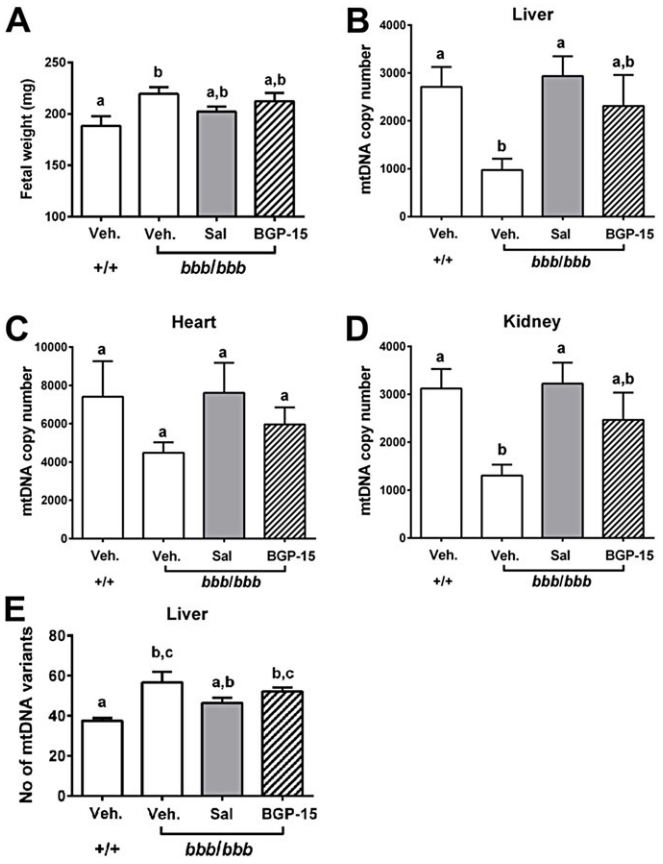

Fig. 7. Altered fetal outcomes of oocytes from obese Blobby mice are alleviated after treatment with salubrinal or BGP-15. Obese mice (*bbb*/*bbb*) and lean littermates (+/+) were treated with vehicle (Veh; saline), salubrinal (Sal) or BGP-15 for 4 days, followed by the isolation of oocytes from oviducts and fertilization by using IVF. Blastocysts were collected at day 5 of culture and transferred to non-obese pseudo-pregnant recipient mice with six blastocysts per uterine horn. On embryonic day 14.5, fetuses were collected and weighed (A). Liver (B), heart (C) and kidney (D) were dissected and the relative mtDNA copy number normalized to β-actin nuclear DNA was determined. Data are presented as means+s.e.m.; lean+Veh, n=18 fetuses from six surrogates; Blobby+Veh, n=20 fetuses from six surrogates; Blobby+Sal, n=22 fetuses from six surrogates; Blobby+BGP-15, n=15 fetuses from four surrogates. (E) Liver mtDNA samples (n=4 fetuses from each treatment group) were analyzed by using next generation sequencing, and rearrangements were identified. Different letters indicate significant differences calculated by one-way ANOVA, Tukey's post hoc test; P<0.01.

(Fig. 7E). Offspring from the oocytes of obese mice that had been treated with salubrinal or BGP-15 harbored 46.5±2.6 and 51.2±2.1 rearrangements, respectively (Fig. 7E). The majority of the rearrangements were single base-pair deletions, mainly detected at levels <10% (supplementary material Table S1). The most affected gene was Complex I of the electron transfer chain with each of the mtDNA-encoded subunits affected. Thus, offspring conceived from the oocytes of obese mothers exhibit alterations in both mtDNA content and variant frequency compared with those from non-obese mothers.

DISCUSSION

Obese women have a well-known risk for anovulation and reduced pregnancy rates (Gesink Law et al., 2007; Rittenberg et al., 2011); our data now shows that concerted ER stress responses in both granulosa and cumulus cells, impaired matrix protein production and high levels of spindle abnormalities are likely to be responsible for reduced ovulation and poor fertilization rates in obese animals. Most alarmingly, however, following conception, maternal obesity is also associated with adiposity in offspring (Ruager-Martin et al., 2010), suggesting that metabolic change can be transmitted through the generations in a self-perpetuating cycle that is set by maternal over-nutrition. Our findings confirm that fetal growth is altered in obese mothers and further demonstrate that this developmental trajectory is established during oocyte development and maturation. We show the existence of a mechanism whereby nutrition in mothers, in this case obesity, can alter the embryo and fetal mitochondrial endowment.

These fetal programming outcomes are clearly the result of changes to the oocyte within the follicle or before fertilization in the oviduct, because the study design utilized IVF throughout, with subsequent embryo culture and gestation under identical conditions for obese and control oocytes. Furthermore, the outcomes were reversed using drug treatments applied in the days before conception. Thus, we show that maternal mtDNA transmission is determined by mitochondria in the preconception oocyte, which are extraordinarily sensitive to maternal metabolic status and stress, and that reductions in mtDNA content imparted before implantation are perhaps the root cause of later altered energy expenditure and of predisposition to metabolic disease. This would provide a mechanistic explanation for previous studies that have reported that rats fed obesogenic diets before conception through to lactation have offspring with reduced levels of liver and kidney mtDNA, reduced electron transport chain activity, insulin resistance and altered energy expenditure (Taylor et al., 2005; Bruce et al., 2009; Borengasser et al., 2011; Burgueño et al., 2013).

Salubrinal is a well-characterized and widely used ER stress inhibitor; however, BGP-15 also modulated ER stress pathways, specifically, in obese Blobby mice it decreased COC *Atf4* mRNA to the normal levels seen in lean mice and it also increased *Xbp1*s levels. Treatment with BGP-15 also dramatically increased transcripts of the cytoprotective chaperones *Hspa1a* and *Hspa1b*, consistent with BGP-15-induced expression of HSP72 protein in muscle (Chung et al., 2008; Gehrig et al., 2012), which is likely to be responsible for the increase in *Xbp1*s (Gupta et al., 2010). ER stress inhibitor treatment also improved ER secretory protein production, as evidenced by the expression of PTX3, selected because it is rapidly expressed at high levels in response to the luteinizing hormone surge and is essential for ovulation and fertilization (Varani et al., 2002; Salustri et al., 2004). This reduction in PTX3, and probably other cumulus cell secreted proteins, is likely to be at least partly responsible for the anovulation and decreased *in vivo* fertilization rates seen in obese mice (Fig. 2; Minge et al., 2008; Wu et al., 2010). However, it is equally possible that leptin (or gonadotropin) receptor desensitization occurs in ovarian cells, as occurs in the hypothalamus in response to obesity (Ozcan et al., 2009), or that proteins which are crucial for cumulus cell-oocyte communication and developmental competence, such as gap junctions (Li and Albertini, 2013), are disrupted. ER stress inhibitor treatment did not affect oocyte lipid content, confirming that their mechanism of action is likely to be stabilization of ER protein production and mitochondrial membrane potential, rather than the alleviation of high intracellular lipid. Both compounds reduced autophagy responses; however, they also increased both TFAM and DRP1, indicating amplified mtDNA replication and mitochondrial fission as the mechanism of action to improve oocyte developmental potential. In support of this, mtDNA content does not change markedly in embryos from obese mice in the oocyte to embryo transition; increasing from an average of 2.6×10^5 copies

Development (2015) 142, 681-691 doi:10.1242/dev.114850

to just 4.2×10^5 copies (see Fig. 5E versus Fig. 6E). By contrast, embryos from lean mice increase mtDNA from 2.9×10^5 copies to 12.9×10^5 copies, as is known to occur in preparation for implantation (Pikó and Taylor, 1987; Ebert et al., 1988; Thundathil et al., 2005; Spikings et al., 2007; Aiken et al., 2008; Wai et al., 2010). Importantly, these low mtDNA embryos give rise to fetal tissues that have correspondingly reduced mtDNA content and increased mtDNA sequence variants, reflective of an altered metabolic capacity (Park et al., 2001; Meierhofer et al., 2004; Yuzefovych et al., 2013), which is consistent with their significantly increased fetal weight. That placental tissue from fetuses derived from oocytes of obese mice did not have reduced mtDNA content (or altered tissue weight), suggesting that the reduction in mtDNA in blastocysts mostly impacts cells within the inner cell mass, which establish the set point of tissue-specific mtDNA content as fetal tissues differentiate (Facucho-Oliveira et al., 2007; St John, 2012).

BGP-15 is an orally active compound that is currently in human clinical trials for type II diabetes (Literáti-Nagy et al., 2009, 2010). In a rat model of type II diabetes, BGP-15 increases mitochondrial area in muscle and improves insulin sensitivity (Henstridge et al., 2014), and in a model of acetaminophen-induced liver toxicity, BGP-15 induces phosphorylated eIF2α and restores mitochondrial depolarization (Nagy et al., 2010). The observation that BGP-15 had no effect on mitochondrial replication in oocyte complexes from lean mice was not unexpected because this class of compounds has no discernible effects in the absence of cellular stress (Chung et al., 2008; Nagy et al., 2010; Crul et al., 2013). Our findings that BGP-15 (as well as the laboratory reagent salubrinal) is able to reverse mitochondrial dysfunction in oocytes clearly demonstrate that obesity-induced, and probably other, mitochondrial deficits in oocytes can be alleviated by using interventions before conception to improve embryo and fetal development.

MATERIALS AND METHODS

Study approval

All experiments were approved by the University of Adelaide Animal Ethics Committee and conducted in accordance with the Australian Code of Practice for the Care and Use of Animals for Scientific Purposes.

Animals

Details about the Blobby mutation and genotyping can be found in the supplementary methods. All experimental mice were female and were 14 weeks of age unless otherwise indicated. Mice were injected intraperitoneally (i.p.) with equine chorionic gonadotropin (eCG; National Hormone and Peptide Program, Torrance, CA, USA) at 5 I.U./0.1 ml saline (0.9%) per 12 g of bodyweight, followed 48 h later by i.p. injection of human chorionic gonadotropin (hCG; Merck, Sharp and Dohme) at 5 I.U./0.1 ml saline per 12 g of bodyweight. Salubrinal (Invitrogen) was injected i.p. at 1 mg/kg of bodyweight (Sokka et al., 2007) in approximately 0.1 ml saline daily for four consecutive days starting the day prior to treatment with eCG. BGP-15 (kindly provided by N-Gene Research Laboratories) was injected at 100 mg/kg of bodyweight in saline (Racz et al., 2002) on an identical schedule, which is based on our previous results (Minge et al., 2008).

Metabolite and endocrine measurements

Blood samples were collected from mice immediately before humane killing by cervical dislocation. Samples were allowed to clot at room temperature and centrifuged at 4000 r.p.m. (1800 ***g***) for 10 min, followed by collection of serum. Mice were not fasted to avoid the detrimental physiological impact of short-term starvation on ovulation and oocyte quality. Parametrial adipose tissue and liver were dissected and weighed.

Serum insulin levels were measured by using the sensitive rat insulin RIA kit (Millipore) with a sensitivity of 0.03 ng/ml and an intra-assay coefficient of 7.31%. Serum glucose and lipids were determined by using a Roche Cobas Integra 400 plus chemistry analyzer (Roche). Cholesterol levels were measured using the Cholesterol (CHOL2) assay kit (Roche), and the mean coefficient of variation was less than 2.7%. Triglycerides were measured using a triglycerides (TRIGL) assay kit (Roche), and the mean coefficient of variation was less than 2.6%. Each of these assays was calibrated with the Calibrator for Automated Systems (Roche) and the quality controls were PreciControl ClinChem Multi 1 and PreciControl ClinChem Multi 2 (Roche). Total serum non-esterified fatty acids (NEFAs) were measured using the NEFA-C assay kit (Wako Pure Chemical Industries) and quality controls Seronorm Human and Seronorm Lipid (Sero, Norway). The mean coefficient of variation was less than 4.6%. All assays have been validated for use in the mouse.

Isolation of ovaries and cumulus-oocyte complexes

Ovaries were dissected and fixed in 4% paraformaldehyde (w/v) in PBS [80 mM Na_2HPO_4, 20 mM NaH_2PO_4 and 100 mM NaCl (pH 7.5)] for 24 h and processed into paraffin blocks that were then sectioned (5 µm) and stained with Hematoxylin and Eosin. Images were captured at high resolution using NanoZoomer Digital Pathology technology (Hamamatsu Photonics K.K.). Ovulated cumulus-oocyte complexes (COCs) were isolated from the oviducts of mice at 13 or 16 h after hCG injection as indicated, placed in HEPES-buffered α-MEM (Invitrogen) supplemented with 3 mg/ml bovine serum albumin (fatty acid free; Sigma-Aldrich) and counted under a dissection microscope. Granulosa-lutein cells were obtained by the dissection of ovulated follicles from the ovary, these cells were then snap-frozen.

RNA isolation and real-time reverse transcription (RT)-PCR

Total RNA was isolated from COCs or granulosa-lutein cells and reversed transcribed, as described previously (Wu et al., 2012). Real-time PCR of cDNA was performed in triplicate using SYBR Green PCR Master Mix (Applied Biosystems) and a Rotor-Gene 6000 (Corbett) real-time rotary analyzer. Ribosomal protein L19 was used as a validated internal control for every sample. *Xbp1*s primers were: *Xbp1*s reverse, 5′-AGGCTTGGTGTATACATGG-3′ and *Xbp1*s forward, 5′-GGTCTGCTGAGTCCGCAGCAGG-3′ (Ozcan et al., 2009), and other primers were Quantitect Primer assays (Qiagen). All Primers were shown to have comparable amplification efficiency against the internal control. Real-time PCR data was analyzed using the $2^{-(\Delta\Delta CT)}$ method and expressed as the fold change relative to a calibrator cDNA sample included in each run.

Lipid droplet staining and immunocytochemistry

COCs were fixed for 1 h in 4% paraformaldehyde in PBS with 1 mg/ml polyvinylpyrrolidone (PVP; Sigma), then washed thoroughly in PBS with 1 mg/ml PVP. COCs were then incubated in blocking buffer containing 10% normal goat serum (Vector Laboratories) in PBS for 1 h at room temperature, followed by incubation with a rabbit polyclonal antibody against PTX3 (H-300, sc-32866, Santa Cruz Biotechnology), diluted 1:100 in blocking buffer, overnight at 4°C. After washing in PBS with PVP, COCs were incubated with biotinylated goat-anti rabbit IgG antibody (AP132B, Millipore) 1:1000 in PBS with PVP for 1 h at room temperature. Finally, COCs were washed in PBS with PVP and incubated with 1 ng/ml streptavidin-Alexa Fluor 594 (S32356, Molecular Probes) in PBS with PVP, and then washed thoroughly in PBS with PVP and transferred to 1 µg/ml of the neutral lipid stain BODIPY 493/503 (D-3922, Invitrogen) in PBS with PVP for 1 h in the dark at room temperature before washing thoroughly in PBS with PVP. For spindle staining, oocytes were fixed in 4% paraformaldehyde with 2% Triton X-100 and 1 mg/ml PVP in PBS for 30 min at room temperature, then washed thoroughly in PBS with PVP. Oocytes were then incubated with anti-α-tubulin monoclonal antibody (A11126, Life Technologies) (1:200) for 1 h, followed by donkey anti-mouse IgG Alexa Fluor 488 (A-21202, Millipore) (1:1000) and Hoechst 33342 (Life Technologies; 1 µg/ml) for 30 min, with each step followed by three washes in PBS with PVP. For TFAM and DRP1 detection, fixed oocytes were immunostained with a 1:100 dilution of mouse anti-DRP1 (611112, BD Biosciences), or mouse anti-TFAM (catalog number B01P; Abnova) overnight at 4°C. After washing in PBS with PVP, oocytes were

Development (2015) 142, 681-691 doi:10.1242/dev.114850

incubated with 1:1000 donkey-anti mouse IgG Alexa Fluor 488-conjugated antibody in PBS with PVP with 0.5 µg/ml Hoechst 33342 for 1 h at room temperature in the dark, followed by thorough washing in PBS with PVP. Stained COCs or oocytes were visualized, and images were captured by using a Leica TCS SP5 spectral scanning confocal microscope system (Heerbrugg, Switzerland) using identical magnification and gain settings throughout experiments. Fluorescence intensity was determined using AnalysisPro software (Olympus), whereby a circle was placed over the oocyte (or COC) image, and the sum total of fluorescence within the area was determined. Oocyte spindles were scored as described previously (Choi et al., 2007), where spindle and chromosomal configurations were deemed good (score 1, 2) or abnormal (score 3, 4) based on spindle organization and the degree of chromosomal displacement from the plane of the metaphase plate.

Analysis of oocyte mitochondrial membrane potential (ΔΨm) and autophagy

Oocytes were denuded as described above, and ΔΨm was measured as described previously (Wu et al., 2012). Autophagic vacuoles in live denuded oocytes were visualized using the Cyto-ID Autophagy Detection Kit (Enzo Life Sciences) according to the manufacturer's instructions. Briefly, after washing once with 1× assay buffer, oocytes were incubated with dual-detection solution at 37°C in the dark. Then oocytes were washed once with 1× assay buffer and imaged immediately in green and blue fluorescence channels using a Leica SP5 spectral scanning confocal microscope at identical magnification and gain settings throughout experiments. Using AnalysisPro software (Olympus), a square was placed to cover the oocyte image, and green fluorescence intensity was determined as the sum total of fluorescence in the boxed area.

Quantification of mtDNA copy number and sequence variants

The mtDNA copy number in individual oocytes or blastocysts was quantified absolutely, as described previously (Kameyama et al., 2010). Briefly, oocytes (denuded as above) or day 5 blastocysts were washed with PBS with PVP (1 mg/ml PVP in PBS), collected individually into 1.5 ml siliconized low retention microcentrifuge tubes (Fisher Scientific) with 5 µl of PBS with PVP and stored at −80°C. Genomic DNA was isolated by using the QIAamp DNA micro kit (Qiagen) according to the manufacturer's protocol with carrier RNA (1 µg; Qiagen) added to each sample. Genomic DNA was eluted twice with 50 µl of water and diluted ten times for quantitative PCR. To prepare the quantification standards, a 1186 bp fragment of the 12S ribosomal (r)RNA region of mtDNA was amplified from mouse liver by PCR using the primer pair 5′-ACACCTT-GCCTAGCCA-3′ and 5′-TTTGCCACATAGACGAGTT-3′ with the LongRange PCR kit (Qiagen), and then purified by using the QIAquick PCR purification kit (Qiagen) and cloned using the Qiagen PCR cloning kit (Qiagen). Plasmid DNA was purified from bacteria using Plasmid Maxi kit (Qiagen), and the concentration was determined by using a Nanodrop ND1000 Spectrophotometer (Biolab). Plasmid copy number was calculated as: mass of plasmid (g)=plasmid size (bp)×(1.096×10^{-21} g/bp); mass of plasmid required to generate 1×10^{7} copy number standard stock=1×10^{7}×mass of single plasmid. A standard curve was generated by using seven tenfold serial dilutions ($10^{-1}\times10^{7}$ copies), and standard curve correlation coefficients were consistently greater than 0.98. Real-time quantitative PCR using the primer pair 5′-CGTTAGGTCAAGGTG-TAGCC-3′ and 5′-CCAGACACACTTTCCAGTATG-3′ was performed in triplicate using SYBR green PCR master mix (Applied Biosystems) and a Rotor-Gene 6000. Standard curves were created for each run and sample copy number was generated from the equation of Ct value against copy number for the corresponding standard curve.

DNA was extracted from fixed fetal tissue according to a method modified from one described previously (Rodríguez et al., 2002). Briefly, each dissected tissue was washed with PCR-grade water (Fisher Scientific) three times and then added to 460 µl of extraction buffer (100 mM Tris-HCl, 10 mM EDTA, 100 mM NaCl, 2% SDS, 50 mM dithiothreitol, pH 8; Sigma). Tissues were homogenized by using a disposable tissue grinder pestle followed by the addition of 40 µl of proteinase K (10 mg/ml in sterile water; Sigma) and were then incubated for 12 h at 50°C with gentle shaking. Chloroform (550 µl) was then added, followed by gentle mixing and centrifugation at 14,000 r.p.m. (22,000 ***g***) for 10 min. The aqueous layer was transferred to a fresh Eppendorf tube, and DNA was precipitated by adding 1083 µl absolute ethanol and 153 µl 2 M NaCl (Sigma) before an overnight incubation at −20°C. DNA was pelleted by centrifugation at high speed for 15 min, followed by rinsing the pellet twice with 1 ml of 70% ethanol. After air drying, the pellet was resuspended in 100 µl PCR-grade water.

DNA extracted from fixed fetal tissues was used to estimate average mtDNA copy number per cell as described previously (Aiken et al., 2008). The primers for amplification of the mitochondrial gene (12S rRNA) were as above. The primers for amplification of the nuclear gene (β-actin) were 5′-GGAAAAGAGCCTCAGGGCAT-3′ and 5′-CTGCCT-GACGGCCAGG-3′. Quantitative PCR of mitochondrial DNA and nuclear DNA was performed simultaneously in each sample in triplicate using SYBR green PCR master mix (Applied Biosystems) and a Rotor-Gene 6000 (Corbett) real-time rotary analyzer. The Ct value for β-actin was subtracted from that for 12S rRNA to give the ΔCt value. mtDNA copy number per nuclear genome (two actin gene copies) was calculated as $2\times2^{\Delta Ct}$.

The mtDNA sequence was examined in fetal liver samples by using next generation sequencing, which is detailed in the supplementary methods. Briefly, two overlapping fragments, each spanning 50% of the mitochondrial genome, were produced by using long PCR to generate templates. Purified pairs of amplicons from long PCR from the same sample were combined at equal concentrations. Libraries were generated using the Ion Fragment Library Kit and Ion Xpress Template Kit (Life Technologies) and loaded onto 316 chips for sequencing on the Ion Torrent Personal Genome Machine (PGM). Variant selection was performed using the CLC Genomics Workbench (v7.0.3), and sequences were mapped to a mouse reference genome (AP013031).

In vitro fertilization, embryo development and transfer

Sperm were collected from the caudal epididymis and vas deferens of 8-week-old wild-type male mice and capacitated in fertilization medium (Vitro Cleave; Cook Australia, Brisbane, Australia) for 1 h at 37°C under an atmosphere of 5% CO_2 and 95% air. After sperm capacitation, COCs were isolated from oviducts of mice at 16 h after hCG treatment as above and washed twice in fertilization medium. COCs and 10 µl of sperm (35,000 sperm/ml) were then co-incubated in 90 µl of fertilization medium for 4 h at 37°C under an atmosphere of 5% CO_2 and 95% air. At 4 h after fertilization, the morphology of oocytes (putative zygotes) was assessed visually, with those oocytes showing dark and fragmented cytoplasm indicative of apoptosis (Fig. 6A, black arrows) deemed non-viable, and all viable oocytes were transferred to fresh medium. At 24 h after *in vitro* fertilization (day 2), embryo cleavage and morphology were assessed, and two-cell embryos were classified as 'on time' and transferred to a fresh 20 µl drop of medium (Vitro Cleave). Embryo morphology was assessed on day 5 (96-100 h after fertilization), with blastocysts and hatching blastocysts classified as 'on time' and the percentage of two-cell embryos that achieved on time development was calculated.

Unhatched blastocysts on day 4 following *in vitro* fertilization and embryo culture conditions as above were transferred into pseudo-pregnant CBA×C57BL/6 F1 female mice at 3.5 days post coitum. Six blastocysts were transferred into each uterine horn for each recipient mouse, and the two horns were given different source embryos. Recipients were humanely killed on E14.5, and fetuses were collected and fixed in 4% paraformaldehyde in PBS. The following day, crown-rump length, fetal weight and placental weight were measured. Fetal liver, heart, kidney and placenta were dissected and retained for DNA extraction as described above.

Statistical analysis

All measures are reported as mean±s.e.m. Statistical significance was determined as indicated, by using Student's *t*-test or one-way ANOVA with Bonferroni post hoc tests, as appropriate, using GraphPad Prism version 5.01 for Windows (GraphPad Software). A *P*-value of less than 0.05 was considered statistically significant.

Acknowledgements
We gratefully acknowledge N-Gene Research Laboratories for supplying BGP-15.

Competing interests
M.A.F. is Chief Scientific Officer of N-Gene Research Laboratories Ltd. J.C.S.J. is funded by OvaScience Inc. L.L.W., D.L.R., S.L.W., M.C., T.-S.T., R.J.N., J.C. and R.L.R. have no competing or financial interests to declare.

Author contributions
L.L.W., D.L.R., R.J.N., J.C. and R.L.R. conceived and designed experiments. L.L.W., S.L.W., M.C., T.-S.T. and J.C.S.J. conducted experiments. M.A.F. provided a key reagent and intellectual input. L.L.W., D.L.R., J.C.S.J., J.C. and R.L.R. analyzed the data. L.L.W., D.L.R. and R.L.R. wrote the manuscript.

Funding
This work was supported by grants from the National Health and Medical Research Council of Australia (NHMRC) [APP1061819 to R.L.R. and J.C.; APP1041471 to J.C.S.J.]; The Operational Infrastructure Support Program of the Government of Victoria; and the Women's and Children's Hospital Foundation (to L.L.W.). M.A.F. is a Senior Principal Research Fellow of the NHMRC. R.L.R. is a Career Development Fellow of the NHMRC.

Supplementary material
Supplementary material available online at
http://dev.biologists.org/lookup/suppl/doi:10.1242/dev.114850/-/DC1

References

Aiken, C. E. M., Cindrova-Davies, T. and Johnson, M. H. (2008). Variations in mouse mitochondrial DNA copy number from fertilization to birth are associated with oxidative stress. *Reprod. Biomed. Online* **17**, 806-813.
Arsov, T., Silva, D. G., O'Bryan, M. K., Sainsbury, A., Lee, N. J., Kennedy, C., Manji, S. S. M., Nelms, K., Liu, C., Vinuesa, C. G. et al. (2006). Fat aussie–a new Alström syndrome mouse showing a critical role for ALMS1 in obesity, diabetes, and spermatogenesis. *Mol. Endocrinol.* **20**, 1610-1622.
Borengasser, S. J., Lau, F., Kang, P., Blackburn, M. L., Ronis, M. J. J., Badger, T. M. and Shankar, K. (2011). Maternal obesity during gestation impairs fatty acid oxidation and mitochondrial SIRT3 expression in rat offspring at weaning. *PLoS ONE* **6**, e24068.
Borradaile, N. M., Han, X., Harp, J. D., Gale, S. E., Ory, D. S. and Schaffer, J. E. (2006). Disruption of endoplasmic reticulum structure and integrity in lipotoxic cell death. *J. Lipid Res.* **47**, 2726-2737.
Boyce, M., Bryant, K. F., Jousse, C., Long, K., Harding, H. P., Scheuner, D., Kaufman, R. J., Ma, D., Coen, D. M., Ron, D. et al. (2005). A selective inhibitor of eIF2alpha dephosphorylation protects cells from ER stress. *Science* **307**, 935-939.
Bruce, K. D., Cagampang, F. R., Argenton, M., Zhang, J., Ethirajan, P. L., Burdge, G. C., Bateman, A. C., Clough, G. F., Poston, L., Hanson, M. A. et al. (2009). Maternal high-fat feeding primes steatohepatitis in adult mice offspring, involving mitochondrial dysfunction and altered lipogenesis gene expression. *Hepatology* **50**, 1796-1808.
Burgueño, A. L., Cabrerizo, R., Gonzales Mansilla, N., Sookoian, S. and Pirola, C. J. (2013). Maternal high-fat intake during pregnancy programs metabolic-syndrome-related phenotypes through liver mitochondrial DNA copy number and transcriptional activity of liver PPARGC1A. *J. Nutr. Biochem.* **24**, 6-13.
Cardozo, E., Pavone, M. E. and Hirshfeld-Cytron, J. E. (2011). Metabolic syndrome and oocyte quality. *Trends Endocrinol. Metab.* **22**, 103-109.
Choi, W.-J., Banerjee, J., Falcone, T., Bena, J., Agarwal, A. and Sharma, R. K. (2007). Oxidative stress and tumor necrosis factor-alpha-induced alterations in metaphase II mouse oocyte spindle structure. *Fertil. Steril.* **88**, 1220-1231.
Chung, J., Nguyen, A.-K., Henstridge, D. C., Holmes, A. G., Chan, M. H. S., Mesa, J. L., Lancaster, G. I., Southgate, R. J., Bruce, C. R., Duffy, S. J. et al. (2008). HSP72 protects against obesity-induced insulin resistance. *Proc. Natl. Acad. Sci. USA* **105**, 1739-1744.
Crul, T., Toth, N., Piotto, S., Literati-Nagy, P., Tory, K., Haldimann, P., Kalmar, B., Greensmith, L., Torok, Z., Balogh, G. et al. (2013). Hydroximic acid derivatives: pleiotropic HSP co-inducers restoring homeostasis and robustness. *Curr. Pharm. Des.* **19**, 309-346.
Dumollard, R., Duchen, M. and Carroll, J. (2007). The role of mitochondrial function in the oocyte and embryo. *Curr. Top. Dev. Biol.* **77**, 21-49.
Ebert, K. M., Liem, H. and Hecht, N. B. (1988). Mitochondrial DNA in the mouse preimplantation embryo. *J. Reprod. Fertil.* **82**, 145-149.
Facucho-Oliveira, J. M., Alderson, J., Spikings, E. C., Egginton, S. and St John, J. C. (2007). Mitochondrial DNA replication during differentiation of murine embryonic stem cells. *J. Cell Sci.* **120**, 4025-4034.
Gehrig, S. M., van der Poel, C., Sayer, T. A., Schertzer, J. D., Henstridge, D. C., Church, J. E., Lamon, S., Russell, A. P., Davies, K. E., Febbraio, M. A. et al. (2012). Hsp72 preserves muscle function and slows progression of severe muscular dystrophy. *Nature* **484**, 394-398.
Gesink Law, D. C., Maclehose, R. F. and Longnecker, M. P. (2007). Obesity and time to pregnancy. *Hum. Reprod.* **22**, 414-420.
Girard, D. and Petrovsky, N. (2011). Alström syndrome: insights into the pathogenesis of metabolic disorders. *Nat. Rev. Endocrinol.* **7**, 77-88.
Gupta, S., Deepti, A., Deegan, S., Lisbona, F., Hetz, C. and Samali, A. (2010). HSP72 protects cells from ER stress-induced apoptosis via enhancement of IRE1alpha-XBP1 signaling through a physical interaction. *PLoS Biol.* **8**, e1000410.
Henstridge, D. C., Bruce, C. R., Drew, B. G., Tory, K., Kolonics, A., Estevez, E., Chung, J., Watson, N., Gardner, T., Lee-Young, R. S. et al. (2014). Activating HSP72 in rodent skeletal muscle increases mitochondrial number and oxidative capacity and decreases insulin resistance. *Diabetes* **63**, 1881-1894.
Igosheva, N., Abramov, A. Y., Poston, L., Eckert, J. J., Fleming, T. P., Duchen, M. R. and McConnell, J. (2010). Maternal diet-induced obesity alters mitochondrial activity and redox status in mouse oocytes and zygotes. *PLoS ONE* **5**, e10074.
Jungheim, E. S., Schoeller, E. L., Marquard, K. L., Louden, E. D., Schaffer, J. E. and Moley, K. H. (2010). Diet-induced obesity model: abnormal oocytes and persistent growth abnormalities in the offspring. *Endocrinology* **151**, 4039-4046.
Kameyama, Y., Ohnishi, H., Shimoi, G., Hashizume, R., Ito, M. and Smith, L. C. (2010). Asymmetrical allocation of mitochondrial DNA to blastomeres during the first two cleavages in mouse embryos. *Reprod. Fertil. Dev.* **22**, 1247-1253.
Kaufman, R. J. (1999). Stress signaling from the lumen of the endoplasmic reticulum: coordination of gene transcriptional and translational controls. *Genes Dev.* **13**, 1211-1233.
Kim, I., Xu, W. and Reed, J. C. (2008). Cell death and endoplasmic reticulum stress: disease relevance and therapeutic opportunities. *Nat. Rev. Drug Discov.* **7**, 1013-1030.
Kuo, T.-F., Tatsukawa, H., Matsuura, T., Nagatsuma, K., Hirose, S. and Kojima, S. (2012). Free fatty acids induce transglutaminase 2-dependent apoptosis in hepatocytes via ER stress-stimulated PERK pathways. *J. Cell. Physiol.* **227**, 1130-1137.
Li, R. and Albertini, D. F. (2013). The road to maturation: somatic cell interaction and self-organization of the mammalian oocyte. *Nat. Rev. Mol. Cell Biol.* **14**, 141-152.
Literáti-Nagy, B., Kulcsár, E., Literáti-Nagy, Z., Buday, B., Péterfai, E., Horváth, T., Tory, K., Kolonics, A., Fleming, A., Mandl, J. et al. (2009). Improvement of insulin sensitivity by a novel drug, BGP-15, in insulin-resistant patients: a proof of concept randomized double-blind clinical trial. *Horm. Metab. Res.* **41**, 374-380.
Literáti-Nagy, B., Péterfai, E., Kulcsár, E., Literáti-Nagy, Z., Buday, B., Tory, K., Mandl, J., Sümegi, B., Fleming, A., Roth, J. et al. (2010). Beneficial effect of the insulin sensitizer (HSP inducer) BGP-15 on olanzapine-induced metabolic disorders. *Brain Res. Bull.* **83**, 340-344.
Luzzo, K. M., Wang, Q., Purcell, S. H., Chi, M., Jimenez, P. T., Grindler, N., Schedl, T. and Moley, K. H. (2012). High fat diet induced developmental defects in the mouse: oocyte meiotic aneuploidy and fetal growth retardation/brain defects. *PLoS ONE* **7**, e49217.
Machtinger, R., Combelles, C. M. H., Missmer, S. A., Correia, K. F., Fox, J. H. and Racowsky, C. (2012). The association between severe obesity and characteristics of failed fertilized oocytes. *Hum. Reprod.* **27**, 3198-3207.
Malhotra, J. D. and Kaufman, R. J. (2007). Endoplasmic reticulum stress and oxidative stress: a vicious cycle or a double-edged sword? *Antioxid. Redox Signal.* **9**, 2277-2294.
Meierhofer, D., Mayr, J. A., Foetschl, U., Berger, A., Fink, K., Schmeller, N., Hacker, G. W., Hauser-Kronberger, C., Kofler, B. and Sperl, W. (2004). Decrease of mitochondrial DNA content and energy metabolism in renal cell carcinoma. *Carcinogenesis* **25**, 1005-1010.
Minge, C. E., Bennett, B. D., Norman, R. J. and Robker, R. L. (2008). Peroxisome proliferator-activated receptor-gamma agonist rosiglitazone reverses the adverse effects of diet-induced obesity on oocyte quality. *Endocrinology* **149**, 2646-2656.
Nagy, G., Szarka, A., Lotz, G., Dóczi, J., Wunderlich, L., Kiss, A., Jemnitz, K., Veres, Z., Bánhegyi, G., Schaff, Z. et al. (2010). BGP-15 inhibits caspase-independent programmed cell death in acetaminophen-induced liver injury. *Toxicol. Appl. Pharmacol.* **243**, 96-103.
Ozcan, L. and Tabas, I. (2012). Role of endoplasmic reticulum stress in metabolic disease and other disorders. *Annu. Rev. Med.* **63**, 317-328.
Ozcan, L., Ergin, A. S., Lu, A., Chung, J., Sarkar, S., Nie, D., Myers, M. G., Jr and Ozcan, U. (2009). Endoplasmic reticulum stress plays a central role in development of leptin resistance. *Cell Metabol.* **9**, 35-51.
Park, K. S., Nam, K. J., Kim, J. W., Lee, Y. B., Han, C. Y., Jeong, J. K., Lee, H. K. and Pak, Y. K. (2001). Depletion of mitochondrial DNA alters glucose metabolism in SK-Hep1 cells. *Am. J. Physiol. Endocrinol. Metab.* **280**, E1007-E1014.
Pikó, L. and Taylor, K. D. (1987). Amounts of mitochondrial DNA and abundance of some mitochondrial gene transcripts in early mouse embryos. *Dev. Biol.* **123**, 364-374.
Racz, I., Tory, K., Gallyas, F., Jr Berente, Z., Osz, E., Jaszlits, L., Bernath, S., Sumegi, B., Rabloczky, G. and Literati-Nagy, P. (2002). BGP-15 - a novel poly

(ADP-ribose) polymerase inhibitor - protects against nephrotoxicity of cisplatin without compromising its antitumor activity. *Biochem. Pharmacol.* **63**, 1099-1111.
Rattanatray, L., MacLaughlin, S. M., Kleemann, D. O., Walker, S. K., Muhlhausler, B. S. and McMillen, I. C. (2010). Impact of maternal periconceptional overnutrition on fat mass and expression of adipogenic and lipogenic genes in visceral and subcutaneous fat depots in the postnatal lamb. *Endocrinology* **151**, 5195-5205.
Rittenberg, V., Seshadri, S., Sunkara, S. K., Sobaleva, S., Oteng-Ntim, E. and El-Toukhy, T. (2011). Effect of body mass index on IVF treatment outcome: an updated systematic review and meta-analysis. *Reprod. Biomed. Online* **23**, 421-439.
Rodríguez, D., Bastida, R. and Olsson, P.-E. (2002). DNA extraction from formalin fixed franciscana tissues. *Latin Am. J. Aquat. Mamm.* **1**, 123-128.
Ruager-Martin, R., Hyde, M. J. and Modi, N. (2010). Maternal obesity and infant outcomes. *Early Hum. Dev.* **86**, 715-722.
Salustri, A., Garlanda, C., Hirsch, E., De Acetis, M., Maccagno, A., Bottazzi, B., Doni, A., Bastone, A., Mantovani, G., Beck Peccoz, P. et al. (2004). PTX3 plays a key role in the organization of the cumulus oophorus extracellular matrix and in in vivo fertilization. *Development* **131**, 1577-1586.
Samuelsson, A.-M., Matthews, P. A., Argenton, M., Christie, M. R., McConnell, J. M., Jansen, E. H. J. M., Piersma, A. H., Ozanne, S. E., Twinn, D. F., Remacle, C. et al. (2008). Diet-induced obesity in female mice leads to offspring hyperphagia, adiposity, hypertension, and insulin resistance: a novel murine model of developmental programming. *Hypertension* **51**, 383-392.
Schaffer, J. E. (2003). Lipotoxicity: when tissues overeat. *Curr. Opin. Lipidol.* **14**, 281-287.
Shankar, K., Harrell, A., Liu, X., Gilchrist, J. M., Ronis, M. J. J. and Badger, T. M. (2008). Maternal obesity at conception programs obesity in the offspring. *Am. J. Physiol. Regul. Integr. Comp. Physiol.* **294**, R528-R538.
Shankar, K., Zhong, Y., Kang, P., Lau, F., Blackburn, M. L., Chen, J.-R., Borengasser, S. J., Ronis, M. J. J. and Badger, T. M. (2011). Maternal obesity promotes a proinflammatory signature in rat uterus and blastocyst. *Endocrinology* **152**, 4158-4170.
Shore, G. C., Papa, F. R. and Oakes, S. A. (2011). Signaling cell death from the endoplasmic reticulum stress response. *Curr. Opin. Cell Biol.* **23**, 143-149.
Sokka, A.-L., Putkonen, N., Mudo, G., Pryazhnikov, E., Reijonen, S., Khiroug, L., Belluardo, N., Lindholm, D. and Korhonen, L. (2007). Endoplasmic reticulum stress inhibition protects against excitotoxic neuronal injury in the rat brain. *J. Neurosci.* **27**, 901-908.
Spikings, E. C., Alderson, J. and St John, J. C. (2007). Regulated mitochondrial DNA replication during oocyte maturation is essential for successful porcine embryonic development. *Biol. Reprod.* **76**, 327-335.
Srinivasan, M., Katewa, S. D., Palaniyappan, A., Pandya, J. D. and Patel, M. S. (2006). Maternal high-fat diet consumption results in fetal malprogramming predisposing to the onset of metabolic syndrome-like phenotype in adulthood. *Am. J. Physiol. Endocrinol. Metab.* **291**, E792-E799.
St John, J. C. (2012). Transmission, inheritance and replication of mitochondrial DNA in mammals: implications for reproductive processes and infertility. *Cell Tissue Res.* **349**, 795-808.
Taylor, P. D., McConnell, J., Khan, I. Y., Holemans, K., Lawrence, K. M., Asare-Anane, H., Persaud, S. J., Jones, P. M., Petrie, L., Hanson, M. A. et al. (2005). Impaired glucose homeostasis and mitochondrial abnormalities in offspring of rats fed a fat-rich diet in pregnancy. *Am. J. Physiol. Regul. Integr. Comp. Physiol.* **288**, R134-R139.
Thundathil, J., Filion, F. and Smith, L. C. (2005). Molecular control of mitochondrial function in preimplantation mouse embryos. *Mol. Reprod. Dev.* **71**, 405-413.
Tian, T., Zhao, Y., Nakajima, S., Huang, T., Yao, J., Paton, A. W., Paton, J. C. and Kitamura, M. (2011). Cytoprotective roles of ERK and Akt in endoplasmic reticulum stress triggered by subtilase cytotoxin. *Biochem. Biophys. Res. Commun.* **410**, 852-858.
Van Blerkom, J., Davis, P. W. and Lee, J. (1995). ATP content of human oocytes and developmental potential and outcome after in-vitro fertilization and embryo transfer. *Hum. Reprod.* **10**, 415-424.
Van Blerkom, J., Davis, P., Mathwig, V. and Alexander, S. (2002). Domains of high-polarized and low-polarized mitochondria may occur in mouse and human oocytes and early embryos. *Hum. Reprod.* **17**, 393-406.
Vannuvel, K., Renard, P., Raes, M. and Arnould, T. (2013). Functional and morphological impact of ER stress on mitochondria. *J. Cell. Physiol.* **228**, 1802-1818.
Varani, S., Elvin, J. A., Yan, C., DeMayo, J., DeMayo, F. J., Horton, H. F., Byrne, M. C. and Matzuk, M. M. (2002). Knockout of pentraxin 3, a downstream target of growth differentiation factor-9, causes female subfertility. *Mol. Endocrinol.* **16**, 1154-1167.
Wai, T., Ao, A., Zhang, X., Cyr, D., Dufort, D. and Shoubridge, E. A. (2010). The role of mitochondrial DNA copy number in mammalian fertility. *Biol. Reprod.* **83**, 52-62.
Wu, L. L.-Y., Dunning, K. R., Yang, X., Russell, D. L., Lane, M., Norman, R. J. and Robker, R. L. (2010). High-fat diet causes lipotoxicity responses in cumulus-oocyte complexes and decreased fertilization rates. *Endocrinology* **151**, 5438-5445.
Wu, L. L., Russell, D. L., Norman, R. J. and Robker, R. L. (2012). Endoplasmic reticulum (ER) stress in cumulus-oocyte complexes impairs pentraxin-3 secretion, mitochondrial membrane potential (DeltaPsi m), and embryo development. *Mol. Endocrinol.* **26**, 562-573.
Yan, X., Huang, Y., Zhao, J.-X., Long, N. M., Uthlaut, A. B., Zhu, M.-J., Ford, S. P., Nathanielsz, P. W. and Du, M. (2011). Maternal obesity-impaired insulin signaling in sheep and induced lipid accumulation and fibrosis in skeletal muscle of offspring. *Biol. Reprod.* **85**, 172-178.
Yuzefovych, L. V., Musiyenko, S. I., Wilson, G. L. and Rachek, L. I. (2013). Mitochondrial DNA damage and dysfunction, and oxidative stress are associated with endoplasmic reticulum stress, protein degradation and apoptosis in high fat diet-induced insulin resistance mice. *PLoS ONE* **8**, e54059.